



Article

## Geodetic monitoring of building deformations based on total station and GNSS measurements in the city of Kentau

Rustem Akhmetov<sup>1</sup>, Zhanar Bimurat<sup>1,2</sup>, Aminyam Baltiyeva<sup>1</sup>, Gulmira Makhmetova<sup>1,\*</sup>

<sup>1</sup>Rock Pressure Laboratory, D.A. Kunaev Institute of Mining, Almaty, Republic of Kazakhstan

<sup>2</sup>Department of Mathematical Computer Modeling, International Information Technology University, Almaty, Republic of Kazakhstan

\*Correspondence: [gmakhmetova@igd.com.kz](mailto:gmakhmetova@igd.com.kz)

**Abstract.** Abstract. This study evaluates building deformation in Kentau, Kazakhstan, a post-mining urban area affected by subsidence and flooded underground workings. Two geodetic observation cycles were conducted in May and October 2025 for 14 residential and administrative buildings using GNSS-referenced total station measurements. Reflective markers installed on building corners were observed with a Leica TS10 total station, while local control networks were tied to the city GNSS framework and adjusted in a unified WGS84-based coordinate system. Inter-cycle displacements were then assessed using positional and vertical errors and compared with normative tolerance levels. Valid repeated measurements were obtained for 26 markers on 11 buildings. Approximately 85% of the markers showed planimetric displacement magnitudes below 20 mm, and about 70% showed vertical displacements within  $\pm 5$  mm. Localized anomalies were recorded at individual markers, including planimetric displacement up to 74.8 mm and vertical displacement values of +616.3 mm and  $-122.7$  mm. The three-marker analysis of building No. 10 indicated differential vertical movement between corners. The results show that GNSS-referenced total station monitoring can provide useful building-scale deformation information in post-mining urban areas, while detected outliers require marker verification, engineering inspection, and continued multi-cycle monitoring.

**Keywords:** geodetic monitoring, building deformation, total station survey, GNSS, mining subsidence.

### 1. Introduction

Kentau is a mining-affected city in southern Kazakhstan where ground and structural deformations develop as post-closure processes linked to the shutdown of underground operations and progressive flooding of mine workings. A principal geodynamic driver within the built-up area is the flooded Mirgalimsay deposit, whose galleries were repeatedly inundated from karst cavities filled with sandy-clayey material during industrial operation [1]. While an active dewatering system maintained low groundwater levels and limited geomechanical disturbance, complete dewatering shutdown on 18 October 2002 altered the hydrogeological regime, leading to rock saturation, strength reduction, and activation of post-closure deformation processes [2]. Persistent underground voids and zones of disrupted rock continuity pose continuing hazards: self-collapse may reactivate rock movement and surface subsidence, adversely affecting buildings and utilities [3]. Under such conditions, systematic deformation monitoring is an essential component of urban geodynamic assessment.

Engineering geodesy offers a well-established toolkit for structural displacement control. Terrestrial geodetic techniques, particularly electronic total station observations to discrete control points, provide object-scale three-dimensional coordinates at millimeter to centimeter precision when redundant observation schemes are applied [4], [5]. Complementary methods such as precise levelling and terrestrial laser scanning are widely used in deformation monitoring but were outside the scope

of the present campaign. Global Navigation Satellite System (GNSS) techniques deliver georeferenced time series of control points and are widely used for regional geodynamic networks and large engineering structures [6], [7], [8]. Nevertheless, GNSS building monitoring exhibits known limitations: reduced sensitivity to small vertical movements, multipath in dense urban environments, and dependence on stable monumentation [7], [9]. Interferometric Synthetic Aperture Radar (InSAR), including Persistent Scatterer and Small Baseline Subset variants, complements point-based geodesy by mapping spatially continuous ground motion; recent applications in Kazakhstan document tectonic and anthropogenic deformation around Almaty and support predictive geodynamic modelling [10], [11]. Mining subsidence literature [2], [12] further emphasizes that technogenic ground movement is spatially heterogeneous and may combine subsidence, heave, and uneven settlement, requiring multi-sensor integration rather than single-technique interpretation.

Integrated monitoring frameworks that combine GNSS, total station observations, remote sensing, and geospatial databases are increasingly proposed for technogenic landscapes, open-pit mines, and subsidence-prone urban districts [12], [13], [14]. In seismic regions of Central Asia, cyclic total station GNSS campaigns on engineering structures have been used to evaluate planimetric and vertical response under complex soil-structure interaction [5], [15]. Three-point or multi-corner marker schemes on buildings enable detection of rigid-body translation, uneven settlement, and orientation change when coordinates are adjusted in a statistically tested reference frame [5,15]. Methodology guidance for accuracy evaluation, least-squares adjustment, and comparison with normative tolerance levels is codified in engineering surveying texts and national standards for geotechnical monitoring [9], [16], [17].

Despite this broader methodological base, relatively few studies validate integrated GNSS-total station building monitoring under the specific post-mining subsidence conditions of Kentau. Regional InSAR and GNSS investigations describe ground-motion patterns at city scale [2], [10], yet building-level validation with repeatable terrestrial networks remains limited. Observation layouts proposed for generic disturbance zones are seldom tested against actual urban fabric affected by flooded workings. Existing Kentau-related work concentrates on karst hazard assessment and deposit-scale geodynamics [1], [2], but does not systematically report inter-cycle building displacements referenced to WGS84 and evaluated against published tolerance levels. Accordingly, this study addresses three gaps: 1) Operational verification of a GNSS-referenced, three-marker total station scheme on multiple buildings in an active technogenic subsidence zone; 2) Quantitative inter-cycle displacement analysis with explicit positional error and vertical error reporting after network adjustment; 3) Comparison of observed movements with tolerance levels prescribed for geotechnical monitoring [17].

The working hypothesis is that integration of GNSS control with redundant total station observations enables more reliable separation of local structural deformation from network noise than either technique applied independently. The objective is to apply this integrated geodetic approach to quantitatively evaluate planimetric and vertical inter-cycle deformations of buildings in Kentau and to interpret the results in the context of contemporary deformation-monitoring practice.

## **2. Materials and Methods**

### *2.1 Study area and monitored objects*

Two geodetic observation cycles were executed in May and October 2025 across the built-up area of Kentau, Kazakhstan. The monitoring program covered 14 buildings of varied functional use, predominantly low- to mid-rise residential and administrative, with masonry and reinforced-concrete structural schemes typical of the Soviet-era mining-town urban fabric (generally two to five stories, rectangular footprints, plastered or brick facade surfaces). Fieldwork was conducted by personnel of the D.A. Kunaev Institute of Mining, Almaty, Kazakhstan. Figure 1 shows the spatial distribution of monitored buildings within the city.

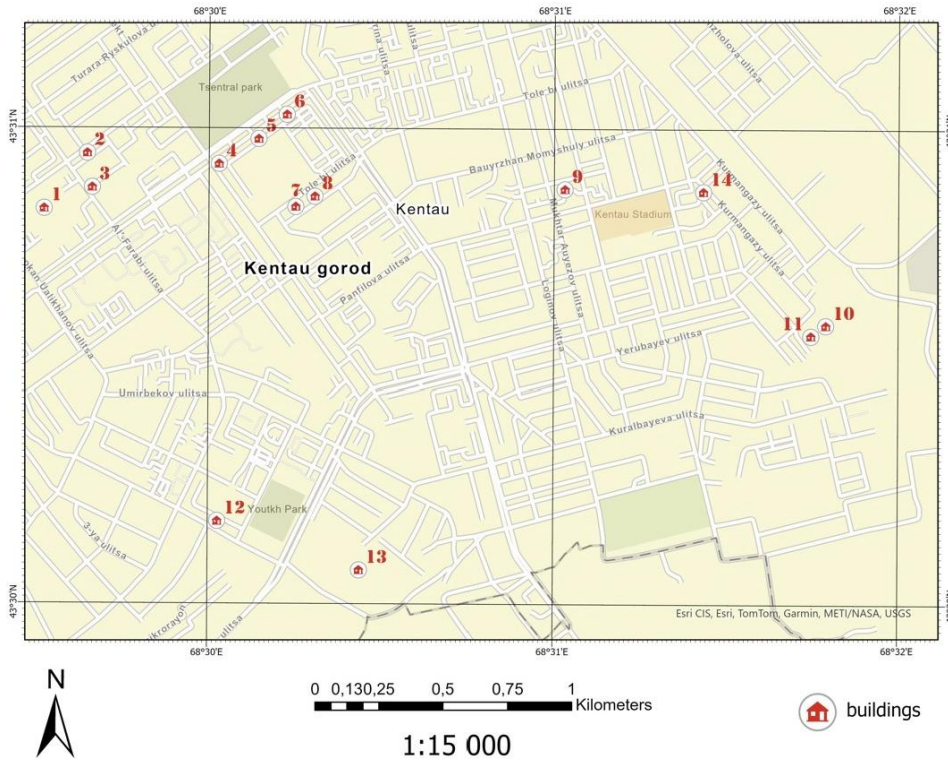


Figure 1 – Location of buildings included in the Kentau deformation monitoring program

### 2.2 Geodetic network design and coordinate system

An integrated methodology combining total station observations and GNSS monitoring was adopted in accordance with established deformation-monitoring practice in complex engineering-geological settings [4], [13]. Figure 2 presents the observation geodetic network deployed across the study area.

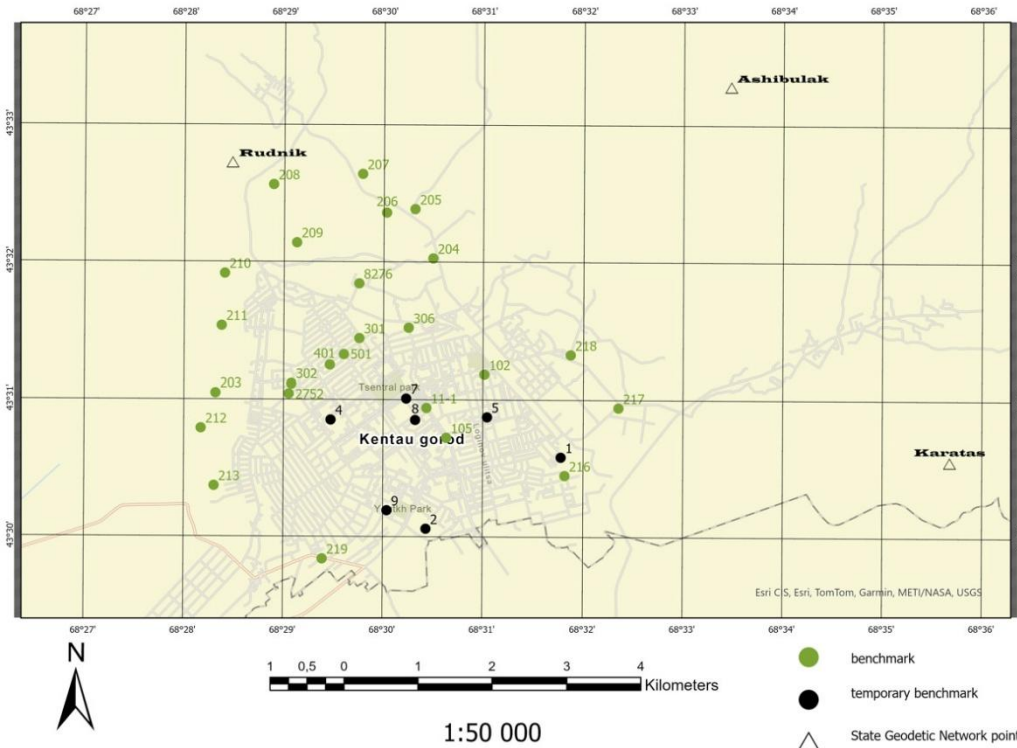


Figure 2 – Schematic of the geodetic monitoring network in Kentau, showing local total station networks, temporary benchmarks, and connection to the city GNSS framework

Near each investigated building, a local total station network with temporary benchmarks was established to ensure repeatability between cycles. The network was initially defined in a local topocentric coordinate system tied to a main instrument station established on stable open ground adjacent to the building. Coordinates of temporary benchmarks were determined from static GNSS observations using dual-frequency receivers. Session duration was not uniform across the network: at individual monitoring points, receivers operated in static mode for 2–5 h, depending on the point observed, while continuously logging carrier-phase and code data. One benchmark per building was integrated into the city GNSS network and designated as the main (reference) station for that object. This station served two functions:

- 1) Linking local total station vectors to a global geodetic frame;
- 2) Detecting potential absolute site shifts between observation cycles [6], [12].

Geodetic integration proceeded as follows. GNSS baseline solutions were computed in WGS84 (EPSG:4326 for geodetic latitude/longitude; projected processing used a local UTM-compatible metric frame consistent with the city GNSS reference). Total station observations were reduced in the local system and transformed to WGS84-compatible metric coordinates using a three-dimensional similarity transformation (translation, rotation, and scale) constrained by the GNSS-derived coordinates of the main benchmark. All total station and GNSS observations from both cycles were finally adjusted in a unified WGS84-based coordinate system so that inter-cycle coordinate differences refer to a common reference frame. Office processing, including total station network adjustment, GNSS baseline computation, coordinate transformation, and variance analysis, was performed with Leica Infinity survey software (version 4.3, Leica Geosystems AG, Heerbrugg, Switzerland).

Figure 3 illustrates a typical temporary GNSS benchmark used for network referencing.



Figure 3 – Temporary GNSS benchmark

### 2.3. Three-marker deformation monitoring scheme

To record building deformations, three reflective deformation markers were installed on each structure following a corner-control configuration widely applied in engineering geodesy [5], [15]. Markers were fixed directly to the load-bearing facade surfaces at building corners using adhesive mounts compatible with repeated sighting. The geometric layout was defined as follows:

- Two markers on the facade (typically the long side facing the primary instrument approach);
- One marker on an adjacent facade meeting at a corner;

– All three markers placed at upper-floor or parallel level where practicable, on externally visible wall surfaces unobstructed by vegetation, balconies, or adjacent structures.

This configuration was selected for four reasons. First, three non-collinear points minimally constrain planimetric translation, vertical displacement, and rotation in the horizontal plane. Second, corner locations maximize structural representativeness for rigid-body tilt and differential settlement. Third, the two-plus-one layout ensures that at least two markers remain visible from any single instrument station, while the third remains observable from an alternate station on the opposite side of the building. Fourth, corner-mounted markers on exterior walls provide direct line-of-sight access for the total station without interior occupancy constraints, critical for operational monitoring in inhabited urban blocks.

Figure 4 shows the marker arrangement relative to the stations and temporary benchmarks.

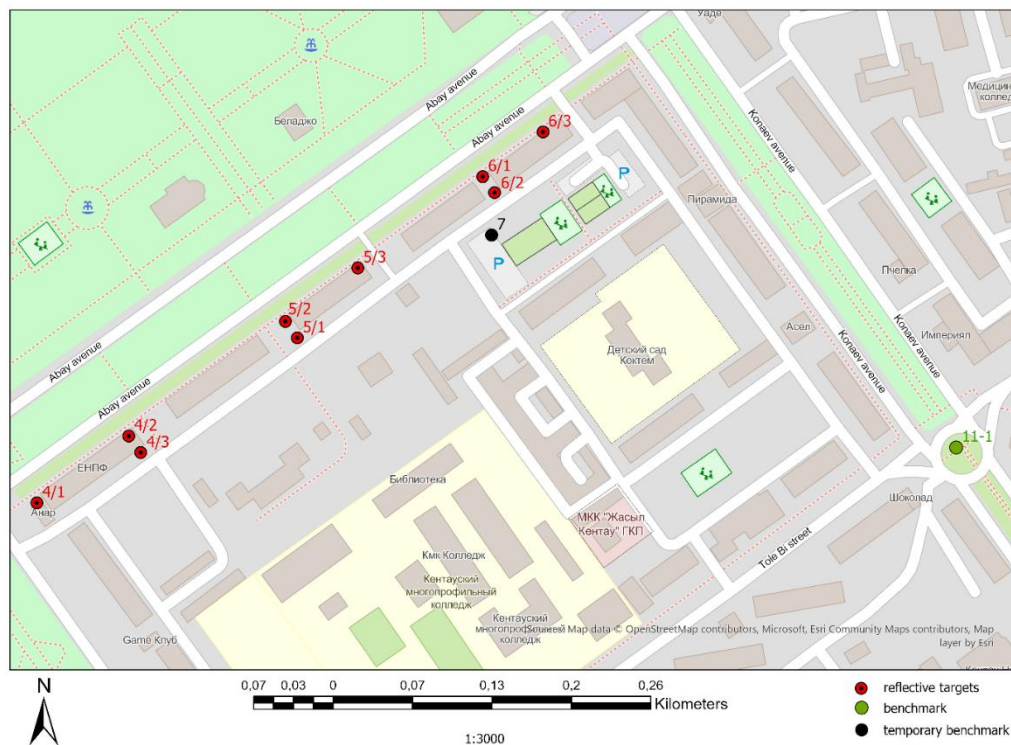


Figure 4 – Layout of three deformation markers on building corners (two markers on one facade, one on the adjacent facade), temporary benchmarks, and total stations ensuring direct line-of-sight visibility: point labels follow the field notation used in the monitoring network; designations with a slash (e.g., 4/1, 4/2, 4/3) identify reflective targets (deformation markers), whereas designations with a hyphen (e.g., 11-1) identify benchmarks

#### 2.4. Field observation procedure

Total station observations were performed with a Leica TS10 electronic total station (angular accuracy 1", Leica Geosystems AG, Heerbrug, Switzerland), an instrument class suitable for building deformation monitoring [5], [12]. Observations were organized sequentially from different sides of each building to guarantee visibility of all three markers:

- 1) The instrument was set up at the main station on the side offering clear sight lines to the two markers on the primary facade; face-left and face-right observations were completed with six rounds per marker, and mean directions and distances were computed.
- 2) The instrument was then moved to a secondary station on the opposite or adjacent side to observe the third marker and to provide independent check observations where geometry permitted.
- 3) Local benchmark points were observed in the same session to maintain network closure.
- 4) Observations from all stations were compared and adjusted jointly, with coordinates referred to the main (GNSS-linked) station as the primary reference for the building network.

Each marker was observed six times in both face-left and face-right positions to suppress collimation, pointing, and eccentricity errors [5], [18]. The three-marker geometry enabled detection of planimetric shifts, vertical displacements, and changes in building orientation between cycles [5].

### 2.5. Data processing, accuracy assessment, and tolerance levels

After least-squares adjustment of the combined total station and GNSS network, the accuracy of each deformation marker was evaluated using standard error-propagation expressions [9], [15], [16].

The horizontal positional error was computed as:

$$S_{xy} = \sqrt{S_x^2 + S_y^2}, \quad (1)$$

where:  $S_x$  and  $S_y$  are the standard deviations (root mean square errors or RMSE) of the adjusted planimetric coordinates of the marker [9], [15].

The vertical error was computed as:

$$S_h = \sqrt{D_h}, \quad (2)$$

where:  $D_h$  is the variance of the adjusted elevation obtained from the least-squares adjustment [16].

Eqs. (1) and (2) express the propagation of adjusted coordinate uncertainties for uncorrelated horizontal components and the height component, respectively, and are standard metrics in geodetic monitoring quality reporting [9], [15].

Inter-cycle displacements between observation cycles  $i$  and  $i - 1$  were calculated as coordinate differences:

$$\Delta X = X_i - X_{i-1}, \Delta Y = Y_i - Y_{i-1}, \Delta H = H_i - H_{i-1}, \quad (3)$$

where:  $X_i$ ,  $Y_i$ ,  $H_i$ , and  $X_{i-1}$ ,  $Y_{i-1}$ ,  $H_{i-1}$  are the adjusted coordinates of the marker in the current and previous cycles [15], [18].

The resultant planimetric displacements magnitude was obtained as:

$$\Delta S_{xy} = \sqrt{(\Delta X)^2 + (\Delta Y)^2}, \quad (4)$$

where:  $\Delta X$  and  $\Delta Y$  are the planimetric coordinate increments between consecutive cycles [18].

Deformation significance was assessed by comparing inter-cycle displacements  $\Delta X$ ,  $\Delta Y$ ,  $\Delta H$ , and  $\Delta S_{xy}$  with tolerance levels prescribed for geotechnical monitoring of buildings and structures. In this study, the comparative normative framework was [17], which defines allowable displacement increments and monitoring accuracy requirements for building safety control [17]. For each marker, measured displacements were evaluated against the corresponding tolerance levels tabulated in [17] for planimetric and vertical displacement control, accounting for building category and observation stage. Displacements exceeding both the adjusted “positional error” or “vertical error” (Eqs. (1) and (2)) and the normative tolerance level were flagged for detailed engineering review. Terminology is applied consistently throughout: positional error and vertical error describe coordinate precision after adjustment; tolerance level denotes the normative allowable displacement threshold; displacement and distribution refer to inter-cycle movement statistics across the marker population.

## 3. Results

Processed total station and GNSS observations yielded planimetric and vertical displacements for all surveyed buildings. For most markers, horizontal positional error remained within approximately 10–20 mm, whereas vertical error was on the order of a few millimeters, supporting reliable detection of vertical movement at the building scale.

Figures 6 and 7 present the distribution of inter-cycle displacements for all deformation markers with valid May–October 2025 comparisons across the monitored building stock ( $n = 26$  markers on 11 buildings; the remaining markers could not be reoccupied in October 2025). These diagrams aggregate every successfully measured marker, not a single building subset. Figures 5 and 6 depict the displacement magnitudes  $\Delta S_{xy}$  and  $\Delta H$ , as given by Eqs. (3) and (4).

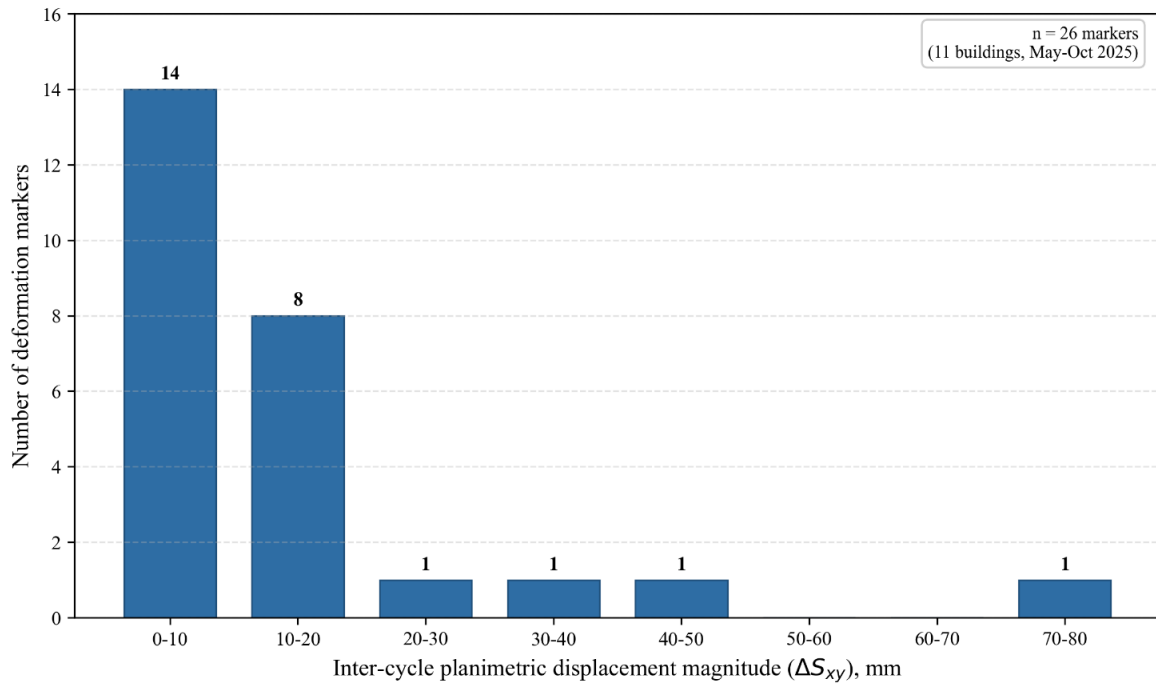


Figure 5 – Distribution of inter-cycle planimetric displacement magnitude  $\Delta S_{xy}$

As shown in Figure 5, the distribution of  $\Delta S_{xy}$  is strongly skewed toward small values: approximately 85% of all monitored markers exhibited planimetric displacement magnitudes below 20 mm. Notable outliers include marker 1/2 ( $\Delta S_{xy} = 74.8$  mm) and 2/1 ( $\Delta S_{xy} = 40.3$  mm).

Figure 6 presents the corresponding distribution of vertical displacement  $\Delta H$ . Roughly 70% of markers fall within the  $\pm 5$  mm range, indicating predominantly stable vertical behavior at the network scale. The distribution is strongly influenced by extreme values at individual corners, including  $\Delta H = 616.3$  mm at marker 2/3 and  $\Delta H = -122.7$  mm at marker 10/2.

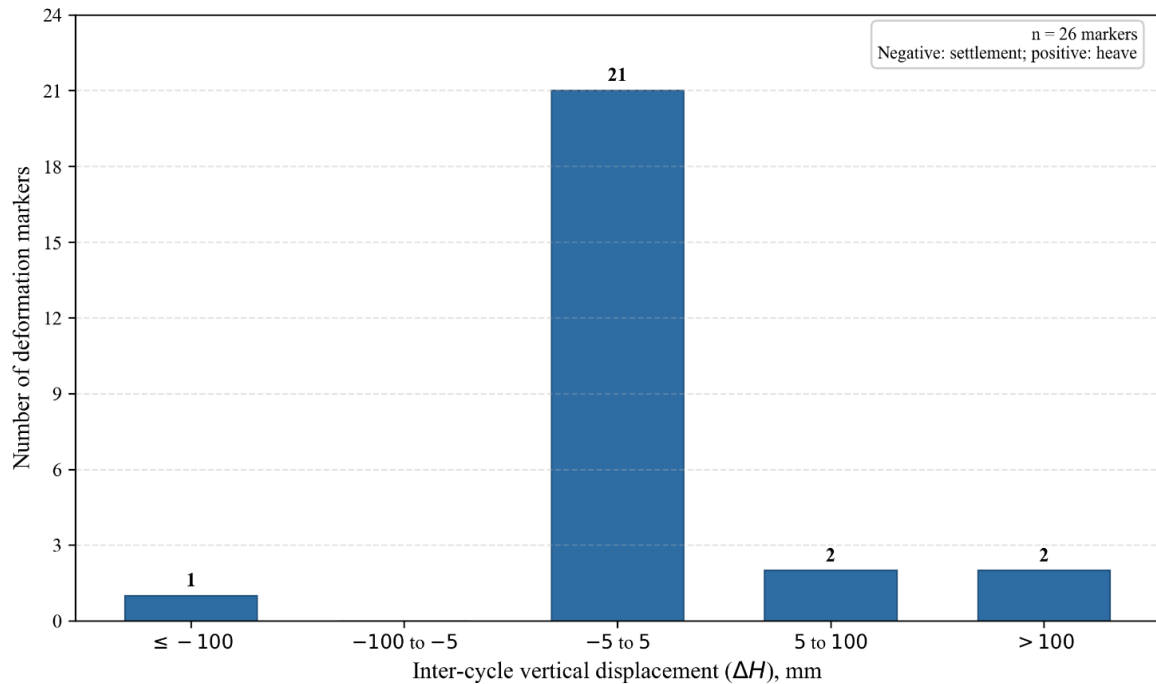


Figure 6 – Distribution of inter-cycle vertical displacement  $\Delta H$

The largest structurally interpretable vertical contrast was recorded at three markers on point 10, with inter-cycle displacements shown in Table 1.

Table 1 – Inter-cycle displacements of deformation markers on building No. 10

Marker	Displacement, mm		
	$\Delta X$	$\Delta Y$	$\Delta H$
10/1	-8.8	-4.7	131.3
10/2	-8.1	-5.2	-122.7
10/3	4.2	11.9	2.2

Figure 7 presents the temporal evolution of elevation changes for the three markers between May and October 2025.

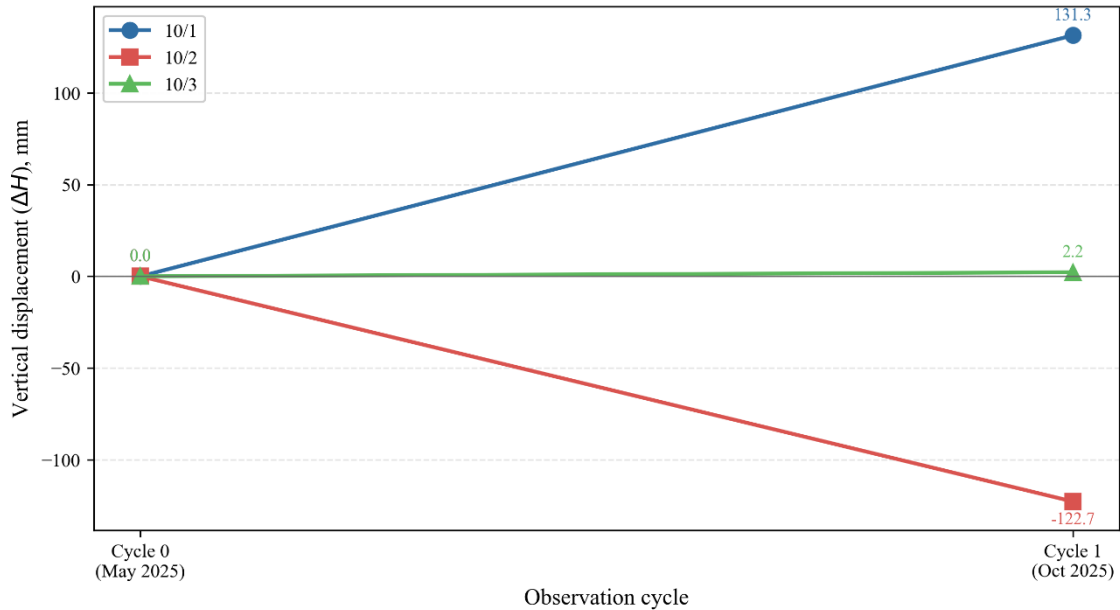


Figure 7 – Temporal development of vertical displacement at deformation marker 10

For the other monitored buildings, consolidated inter-cycle values are presented in Table 2 on a selective basis, retaining only markers with significant displacement amplitudes and excluding cases of negligible, geometrically similar movement.

Table 2 – Selected significant vertical displacements of deformation markers in Kentau

Marker	Displacement $\Delta H$ , mm
1/2	6.0
2/1	5.5
2/3	616.3

During the October 2025 cycle, repeated measurements could not be completed at several objects because temporary benchmarks or deformation markers were lost or damaged, reducing the number of directly comparable records from the nominal 42 markers (14 buildings  $\times$  3) to 26.

## 4. Discussion

### 4.1. Interpretation of network-scale behavior

The aggregated displacement distributions (Figures 5 and 6) indicate that most markers on most buildings remained stable between May and October 2025. Approximately 85% of all valid marker records exhibited  $\Delta S_{xy} < 20$  mm, and roughly 70% showed  $|\Delta H| \leq 5$  mm. This pattern is consistent with slow, spatially differentiated tectonic deformation rather than city-wide catastrophic movement – a finding aligned with regional InSAR and GNSS studies reporting heterogeneous subsidence and local uplift pockets in Kentau rather than uniform basin-scale settlement [2], [10].

The extreme vertical outlier at marker 2/3  $\Delta H = 616.3$  mm and the large opposing vertical components at markers 10/1 and 10/2 requires cautious interpretation. Values of this magnitude within a five-month window exceed typical elastic building response and likely reflect local foundation disturbance, possible marker instability, or unresolved datum effects at individual corners rather than uniform building subsidence alone. Such outliers underscore the value of the three-marker scheme: single-point monitoring would mischaracterize structural behavior, whereas corner arrays expose differential patterns indicative of tilting or local ground failure [5], [15].

For the majority of markers where  $|\Delta H|$  remained within a few millimeters and  $\Delta S_{xy}$  below 20 mm, displacements were comparable to or smaller than normative tolerance levels in [17] when applied to operational monitoring of existing structures [17]. Where displacements exceeded tolerance levels, notably at selected markers at points 2 and 10, engineering follow-up, including inspection, marker verification, and densification of observations, is warranted.

#### 4.2. Comparison with previous studies

Relative to GNSS-dominated high-rise monitoring in seismically active cities [7], [8], the present work emphasizes terrestrial corner control better suited to low- to mid-rise masonry buildings where rooftop GNSS mounting is impractical, and multipath is severe. Compared with InSAR-only regional assessments [10,11], the total station network provides building-resolved, three-dimensional corner displacements at monthly-to-seasonal cadence, albeit at sparse spatial density. This complementarity mirrors integrated frameworks proposed for technogenic objects combining InSAR reconnaissance with total station and GNSS control benchmarks [12], [13].

[6] demonstrated combined GNSS and total station monitoring of engineering structures in seismic regions of Kazakhstan, reporting millimeter-scale accuracy for stable objects, consistent with our adjusted positional error (approximately 10–20 mm at the 95% confidence level for planimetric components) and vertical error (a few millimeters). [5] showed that redundant face measurements and corner marker geometry improve detection of subtle tilting in heritage structures; the six-round face-left/face-right procedure adopted here follows the same principle. [15] emphasize that deformation interpretation must follow formal network adjustment and variance testing; our explicit use of Eqs. (1) and (2) before the displacement analysis adheres to that recommendation.

#### 4.3. Methodological strengths and limitations

The methodological strengths of the study include reproducible three-marker geometry with a documented line-of-sight strategy, GNSS anchoring of each local network in WGS84, redundant total station observations, and explicit comparison with normative tolerance levels [17].

At the same time, the study has several limitations. Only two observation cycles were conducted over five months, which is insufficient to resolve long-term velocity or seasonal effects. In addition, the loss of 16 markers and several benchmarks in October 2025 introduced selection bias in the aggregated distributions. Another limitation is the absence of concurrent InSAR extraction at building corners, which limited regional corroboration of local outliers. Possible conflation of ground and structural components without subsurface profiling at outlier locations should also be considered [1], [2].

Future work should extend the time series over multiple years, integrate Sentinel-1 InSAR velocities with corner displacements, implement automated statistical testing between epochs, including variance-ratio and global congruency tests [15], and replace temporary dowel benchmarks with forced-centering monuments where long-term monitoring is approved [10].

## 5. Conclusions

1. An integrated geodetic monitoring workflow combining GNSS-referenced total station networks, three-marker corner control, and least-squares adjustment in a unified WGS84-based

coordinate system was implemented for building deformation monitoring in the mining-affected city of Kentau, Republic of Kazakhstan.

2. The May–October 2025 inter-cycle comparison showed predominantly stable behavior for the valid marker set. Approximately 85% of the markers had planimetric displacement magnitudes below 20 mm, while about 70% showed vertical displacements within  $\pm 5$  mm. This indicates that most monitored buildings did not demonstrate large inter-cycle movements during the observation period.

3. Localized anomalies were detected at individual markers, including planimetric displacement up to 74.8 mm and vertical displacement values reaching 616.3 mm and  $-122.7$  mm. The three-marker analysis of building No. 10 showed differential vertical movement between corners, indicating the need for detailed engineering inspection, marker verification, and continued monitoring of outlier locations.

4. The results confirm that GNSS-referenced total station monitoring can provide useful building-scale deformation information in post-mining urban areas. However, because the study was based on only two observation cycles and part of the original marker network was lost, further multi-cycle monitoring with more durable benchmarks is required to confirm long-term deformation trends and support reliable risk assessment.

### Acknowledgments

This research is funded by the Committee of Industry of the Ministry of Industry and Construction of the Republic of Kazakhstan under program-targeted funding for scientific research for 2024–2026, BR23991563: “Creation of Innovative Resource-Saving Technologies for Mining and Integrated Processing of Mineral and Technogenic Raw Materials”.

### References

- [1] A. Baltiyeva, E. Orynassarova, Z. Bimurat, and G. Makhmetova, “Comprehensive ground-space monitoring of geodynamic processes at the Mirgalimsay deposit,” in *Proceedings of the 25th SGEM International Multidisciplinary Scientific GeoConference 2025*, Albena, Bulgaria: SGEM, 2025, pp. 127–136. doi: 10.5593/sgem2025/2.1/s09.16.
- [2] E. V. Drobinina, S. V. Shcherbakov, D. R. Zolotarev, O. N. Kovin, G. V. Fedorov, and D. A. Inkin, “Assessment of karst hazards within the orogen territories using geophysical methods (on the example of Kentau city and surroundings, Kazakhstan),” *News of the Ural State Mining University*, vol. 65, no. 1, pp. 28–45, 2022, doi: 10.21440/2307-2091-2022-1-28-45.
- [3] A. Behera and K. Singh Rawat, “A brief review paper on mining subsidence and its geo-environmental impact,” *Materials Today: Proceedings*, p. S2214785323020795, 2023, doi: 10.1016/j.matpr.2023.04.183.
- [4] I. S. Gribkova, R. O. Kuzmin, L. A. Shchenyavskaya, and A. A. Panyutishcheva, “Modern methods and devices of geodetic monitoring of buildings and structures,” *Science. Engineering. Technology (polytechnical bulletin)*, no. 2, pp. 44–47, 2023.
- [5] Z. M. Pawlak, I. Wyczałek, and P. Marciniak, “Two Complementary Approaches toward Geodetic Monitoring of a Historic Wooden Church to Inspect Its Static and Dynamic Behavior,” *Sensors*, vol. 23, no. 20, p. 8392, 2023, doi: 10.3390/s23208392.
- [6] D. Kirgizbayeva, M. Nurpeisova, K. Menayakov, T. Nurpeisova, and A. Umirbayeva, “Monitoring deformations of engineering structures in seismic regions,” *Bulletin of Kazakh Leading Academy of Architecture and Construction*, vol. 96, no. 2, pp. 87–97, 2025, doi: 10.51488/1680-080X/2025.2-09.
- [7] D. Paudel, B. Sherchan, and K. P. Bhandari, “A General Review on Application of GNSS for Structural Deformation Monitoring,” in *Proceedings of 12th IOE Graduate Conference*, Kathmandu, Nepal: Tribhuvan University, 2022, pp. 188–196.
- [8] B. B. Imansakipova, Zh. D. Baygurin, and N. B. Imansakipova, “Geodetic observations of high-rise buildings and structures in seismically hazardous areas,” *KazNU Bulletin. Geography series*, vol. 38, no. 1, pp. 44–47, 2014.
- [9] C. D. Ghilani and P. R. Wolf, *Elementary surveying: an introduction to geomatics*, 13th ed. Upper Saddle River, N.J: Pearson Prentice Hall, 2012.
- [10] E. Bayramov, N. Sydyk, S. Nurakynov, A. Yelisseyeva, J. Neafie, and S. Aliyeva, “Advanced Spaceborne InSAR for monitoring tectonic and anthropogenic ground deformation in the seismically sensitive Almaty region, Kazakhstan,” *Advances in Space Research*, vol. 77, no. 1, pp. 118–146, 2026, doi: 10.1016/j.asr.2025.11.083.

- [11] M. Crosetto, O. Monserrat, M. Cuevas-González, N. Devanthery, and B. Crippa, “Persistent Scatterer Interferometry: A review,” *ISPRS Journal of Photogrammetry and Remote Sensing*, vol. 115, pp. 78–89, 2016, doi: 10.1016/j.isprsjprs.2015.10.011.
- [12] V. V. Kazantseva, D. S. Ozhigin, N. Kosarev, A. K. Satbergenova, and S. B. Ozhigina, “Development of complex system of geotechnical monitoring of technogenic objects based on geospatial data,” *Journal of Mining Institute*, vol. 276, no. 1, pp. 142–156, 2025.
- [13] M. M. Abdukarimov, “Analiz zarubezhnogo opyta geodezicheskogo monitoringa deformatsiy gidrotekhnicheskikh sooruzheniy,” vol. 5, no. 2, pp. 18–25, 2026, doi: 10.5281/ZENODO.18231593.
- [14] A. Ferretti, A. Monti-Guarnieri, C. Prati, F. Rocca, and D. Massonnet, *InSAR principles: guidelines for SAR interferometry processing and interpretation*. in ESA TM, no. 19. Noordwijk, the Netherlands: ESA Publications, ESTEC, 2007.
- [15] M. G. Mustafin, A. V. Zubov, and G. E. Vasiljev, “Deformation estimation procedure for monitoring engineering facilities,” *MIAB*, vol. 8, 2025, doi: 10.25018/0236\_1493\_2025\_8\_0\_92.
- [16] C. D. Ghilani and P. R. Wolf, *Adjustment computations: spatial data analysis*, 4th ed. Hoboken, N.J: John Wiley & Sons, 2006.
- [17] “SP 305.1325800.2017 Buildings and structures. The rules of geotechnical monitoring under construction,” Moscow, Russia: Standardinform, 2017, p. 57.
- [18] V. V. Simonian, A. V. Labuznov, N. V. Angelova, and M. S. Savin, “The comparative analysis of methods of range measurements to assess the applicability of these methods for geodetic monitoring of extended objects,” *International scientific, technical and industrial electronic journal «Geo Science»*, no. 3–4, pp. 22–30, 2011.

### Information about authors:

*Rustem Akhmetov* – Junior Researcher, Rock Pressure Laboratory, D.A. Kunaev Institute of Mining, Almaty, Republic of Kazakhstan, [rakhmetov@igd.com.kz](mailto:rakhmetov@igd.com.kz)

*Zhanar Bimurat* – PhD; 1) Leading Researcher, Rock Pressure Laboratory, D. A. Kunaev Institute of Mining, Almaty, Republic of Kazakhstan; 2) Assistant Professor, Department of Mathematical Computer Modeling, International Information Technology University, Almaty, Republic of Kazakhstan, [zhbimurat@igd.com.kz](mailto:zhbimurat@igd.com.kz)

*Aminyam Baltiyeva* – Leading Researcher, Rock Pressure Laboratory, D.A. Kunaev Institute of Mining, Almaty, Republic of Kazakhstan, [geomine.lab@igd.com.kz](mailto:geomine.lab@igd.com.kz)

*Gulmira Makhmetova* – Junior Researcher, Rock Pressure Laboratory, D.A. Kunaev Institute of Mining, Almaty, Republic of Kazakhstan, [gmakhmetova@igd.com.kz](mailto:gmakhmetova@igd.com.kz)

### Author Contributions:

*Rustem Akhmetov* – methodology, resources, testing, data collection, analysis.

*Zhanar Bimurat* – drafting, editing.

*Aminyam Baltiyeva* – data collection, drafting, editing.

*Gulmira Makhmetova* – analysis, interpretation, concept.

**Conflict of Interest:** The authors declare no conflict of interest.

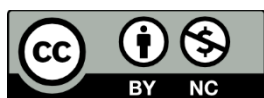
**Use of Artificial Intelligence (AI):** AI assistance was applied to improve language clarity.

*Received:* 04.03.2026

*Revised:* 08.06.2026

*Accepted:* 17.06.2026

*Published:* 22.06.2026



**Copyright:** © 2026 by the authors. Licensee Technobius, LLP, Astana, Republic of Kazakhstan. This article is an open access article distributed under the terms and conditions of the Creative Commons Attribution (CC BY-NC 4.0) license (<https://creativecommons.org/licenses/by-nc/4.0/>).